Preliminary Information on the University of Wisconsin Tandem Mirror Reactor Design

B. Badger, G.L. Kulcinski, L.L. Lao, D.C. Larbalestier, E. Larsen, L-P. Mai, J. Beyer, J.D. Callen, R.W. Conn, G.A. Emmert, S. Grotz, S. Hong, J. Kesner, T.K. Mau, C.W. Maynard, I. Ojalvo, K. Okula, M. Ortman, R.T. Perry, J. Santarius, J. Scharer, K. Shaing, I.N. Sviatoslavsky, D.K. Sze, W.F. Vogelsang, A. White, and P. Wilkes

November 1979

UWFDM-325

FUSION TECHNOLOGY INSTITUTE

UNIVERSITY OF WISCONSIN

MADISON WISCONSIN

Preliminary Information on the University of Wisconsin Tandem Mirror Reactor Design

B. Badger, G.L. Kulcinski, L.L. Lao, D.C. Larbalestier, E. Larsen, L-P. Mai, J. Beyer, J.D. Callen, R.W. Conn, G.A. Emmert, S. Grotz, S. Hong, J. Kesner, T.K. Mau, C.W. Maynard, I. Ojalvo, K. Okula, M. Ortman, R.T. Perry, J. Santarius, J. Scharer, K. Shaing, I.N. Sviatoslavsky, D.K. Sze, W.F. Vogelsang, A. White, and P. Wilkes

Fusion Technology Institute
University of Wisconsin
1500 Engineering Drive
Madison, WI 53706

http://fti.neep.wisc.edu

November 1979

UWFDM-325

Preliminary Information on the University of Wisconsin Tandem Mirror Reactor Design

by

B. Badger, J. B. Beyer, J. D. Callen
R. W. Conn, G. A. Emmert, S. Grotz,
S. O. Hong*, J. Kesner, G. L. Kulcinski,
L. L. Lao, D. C. Larbalestier, E. Larsen,
L-P. Mai, T. K. Mau, C. W. Maynard,
I. Ojalvo**, K. Okula, M. Ortman, R. Perry,
J. Santarius, J. Scharer, K. Shaing,
I. Sviatoslavsky, D. K. Sze, W. F. Vogelsang,
A. White, P. Wilkes

November 2, 1979

UWFDM-325

To be presented at DOE Review of Tandem Mirror Reactor Studies, Washington, DC, November 27-28, 1979.

*AIRCO Central Research Laboratory, Murray Hill, NJ.
**Grumman Aerospace Corporation, Bethpage NY.

Table of Contents

I. Introduction

The recent innovations in plasma confinement for the tandem mirror reactor (TMR) have encouraged scientists and engineers to explore the reactor potential of this concept. The potential for steady state operation, much simpler blanket/shield and magnetic coil design, and the possibility of using direct conversion of the plasma ion energy to electricity are but a few of the major attractions of the TMR. The objective of the Fusion Engineering Program at the University of Wisconsin is to perform a self-consistent conceptual DT tandem mirror reactor design which maximizes Q (the ratio of the fusion energy to the injected energy) while still retaining the economic features of a commercial power plant.

There are four general guidelines for the conceptual reactor design.

1) *The reactor should be a near term commercial reactor (~2020 operation) which utilizes the plasma physics and technology base which is expected to exist shortly after the year 2000.*

2) *The net electrical power level of the reactor should be ~1000 MW_e as opposed to a much smaller proof of principle plant (e.g., a few hundred MW_e) .*

3) *The reactor should employ the optimum combination of RF and neutral beam heating technology, direct conversion of particle energy lost out the ends of the reactor and operate on a steady state basis.*

4) *The main emphasis of the reactor design should be on "credibility" as opposed to choosing techniques or materials that might offer the lowest environmental impact. It is felt that environmental optimization can be accomplished after a "working reactor" configuration has been established.*

In contrast to past Tokamak reactor designs which have been performed by the fusion technology group, the evolution of physics and reactor concepts for the TMR is very dynamic. This has extended the normal process of parametric studies far beyond that required in the Tokamak area

and this report will only summarize the important conclusions that we have reached with respect to "pieces" of the design, e.g., plasma physics, magnets, blankets, etc. We have not yet joined the various components into even a preliminary conceptual design. This is expected to take place in early 1980.

Therefore, the rest of this report will concentrate on 5 important areas of our TMR design activities.

A) Point Code for Reactor Plasma Optimization,

B) New Ideas in Barrier Cell Design,

C) RF Heating Concepts,

D) Magnet Design, and

E) Blanket Considerations.

Since this is only a "snapshot" in our evolution to a more comprehensive design, the reader should treat the following information with the proper amount of caution as it may be significantly altered in the months to come. Finally, the future directions of the TMR Design Studies at Wisconsin will be summarized at the end of this report. The preliminary parameters of the UW Tandem Mirror Reactor are given in Table V-1.

II. Plasma Physics

II-A. Power Balance in a Tandem Mirror Reactor

Although portions of the physics of a tandem mirror reactor with a thermal barrier are as yet under development, much can be gleaned from a simple model. This section sketches the analysis and numerical method used to generate the plasma physics parameters included in this report. Some general aspects of the problem will also be discussed.

The plasma is treated as consisting of four components: 1) electrons trapped in the central cell and electrons passing through both central cell and plug; 2) ions trapped in the central cell; 3) electrons trapped in the plug; and 4) ions trapped in the plug. The electrons of the first component are grouped together because the passing electrons spend most of their time in the central cell and therefore equilibrate in temperature with the central cell electrons. Because the detailed physics of the thermal barrier is uncertain, no separate equations are written for particles in the barrier; the effects of the barrier are treated in a reasonable way which will be described later in this section.

The goals of the analysis were to find parameters for power balance in a tandem mirror with thermal barriers where fusion power output was 3000 MW_{th}, neutron wall loading was two to four MW/m^2, central cell length was less than 100 m, and Q, the ratio power out to power in, was greater than 20. As can be seen from the earlier sections of this report, this was achieved with appropriate caveats which will be discussed later.

The equilibrium power balance equations are solved numerically by taking a set of initial plasma parameters and iterating by time-stepping the temperatures, potentials, and auxiliary electron heating until an equilibrium is reached.

This method is based on that of Shaing, et al.[1]

Since the total fusion power is proportional to the central cell plasma volume and the wall loading is inversely proportional to wall area, specifying these and assuming two alpha particle radii between plasma and wall gives the central cell length and plasma radius. Flux conservation gives plasma radii for the barrier and plug. The plug neutral beam injection energy is specified, as is the cold electron current into the central cell. The detailed magnetic field design and stability analysis have not yet been completed; therefore, central cell beta (the ratio of plasma pressure to magnetic field pressure), plug beta, and magnetic field profile are given quantities, using previous results and physical intuition for guidance.

Because the type of barrier generation method to be used is not yet firmly established, a general approach to the power required is taken. The rate at which passing ions trap in the barrier cell is modelled by:

$$J_{trap} = \frac{n^2_{pass,i}}{5.5x10^9 T_{ic}^{3/2}} \left(1 + .55 \frac{B_{maxb}}{\langle B \rangle_b}\right) \qquad \text{(II.A.1)}$$

which has been fitted to a Fokker-Planck code.[2] Units in all equations are CGS, except energy which is in keV. T_{ic} is the central cell ion temperature;

$$n_{pass,i} = n_c \frac{g_b}{R_b} \left(\frac{T_{ic}}{\pi\phi_b + T_{ic}}\right)^{1/2} \qquad \text{(II.A.2)}$$

is the density of ions streaming through the barrier, which is derived from flux conservation; B_{maxb} is the maximum barrier field; $\langle B \rangle_b$ is the average B field in the barrier assuming a parabolic profile; n_c is the central cell density;

$R_b = B_{maxb}/B_b$; B_b is the minmum barrier field, and ϕ_b is the barrier potential. The barrier pumping parameter, g_b, is the ratio of the total ion density to streaming ion density in the barrier, $n_b = g_b\, n_{pass,i}$, and is a measure of the pumping efficiency; $g_b = 1$ implies perfect pumping. However, the pumping parameter $g_b = 2$ which assumes that as many ions are trapped as are streaming through the barrier, thus assuming some inefficiency in the pumping process. The somewhat pessimistic assumption is made that trapped barrier ions are removed with energy $\phi_b + T_{ic}$ at the rate J_{trap}, and that this amount of energy per unit volume must be replaced as energy input to the plasma. On the other hand, the barrier length, L_b, is taken to be five meters in order to keep the barrier volume and, therefore, pump power low and also to minimize the length of bad magnetic field curvature, thus hopefully helping the central cell beta limit, β_c; details of the magnetic field design and stability analysis are being pursued.

The potential profile is shown in Fig. II-1. The barrier potential ϕ_b is given by flux conservation assuming that the flux at the peak barrier field point is related to n_b by a Boltzmann distribution;

$$\left(\frac{T_{ic}}{\pi\phi_b + T_{ic}}\right)^{1/2} e^{\phi_b/T_{ec}} = \frac{R_b}{g_b} \qquad \text{(II.A.3)}$$

where T_{ec} is the central cell electron temperature.

The potential ϕ_e, which confines the electrons, is given by the particle balance equation

$$\frac{n_c^2}{(n\tau)_{ic}} V_c + \frac{n_c^2}{2} \langle\sigma v\rangle_{DT} V_c + J_{trap}\, 2V_B + f_{is} \frac{n_c^2}{(n\tau)_{ic}} V_c + \frac{n_p^2}{(n\tau)_{ip}} 2V_p = \frac{n_c^2}{(n\tau)_{ec}} V_c \quad \text{(II.A.4)}$$

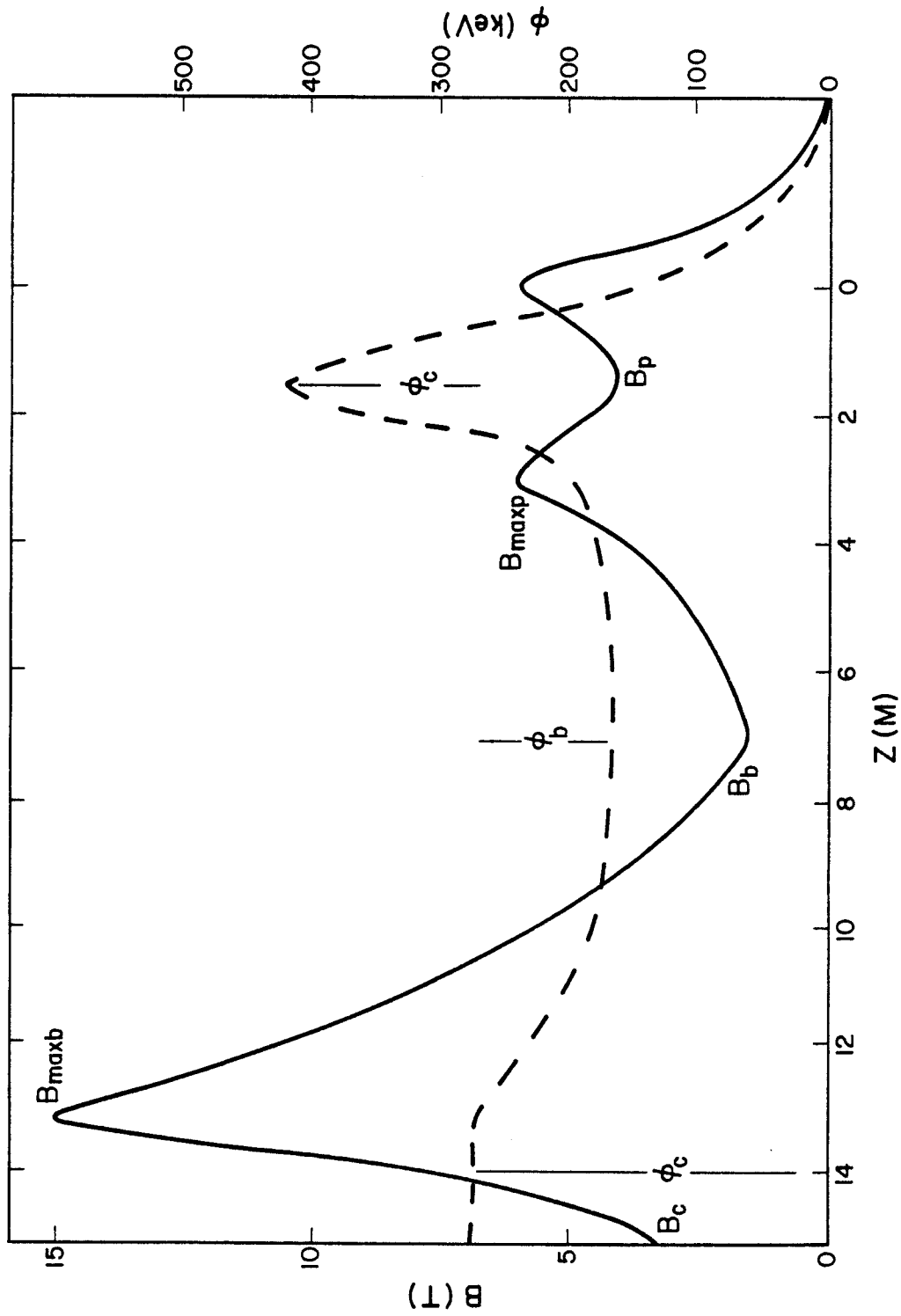
B (T)
Z (M)
φ (keV)
B_{maxb}
B_{maxp}
B_c
B_b
B_p
ϕ_c
ϕ_b
ϕ_c
15
10
5
0
0
2
4
6
8
10
12
14
500
400
300
200
100
0

Fig. II-1

where V_c is the central cell volume; $\langle\sigma v\rangle_{DT}$ is the fusion reaction rate; V_B is the barrier volume; f_{is} the ratio of cold electron to ion ionization current in the central cell, which is used, if desired, to lower the central cell electron temperature and thus raise n_c for a given β_c; and V_p is the plug volume. $(n\tau)_{ic}$ and $(n\tau)_{ec}$ for ions and electrons in the central cell are given Pastukhov formulas as corrected by Cohen, et al.[3,4]

$$(n\tau)_{ac} = \frac{n_c\tau_a}{Z_a}\ \frac{\phi_a}{T_{ac}}\ \frac{G(R_c Z_a)}{I(T_{ac}/\phi_a)}\ e^{\phi_a/T_{ac}} \qquad \text{(II.A.5)}$$

where $n_c\tau_a = m_a\, v_{Ta}^3/(4\pi e^4 \Lambda a)$, m_a is the particle mass, $v_{Ta}=(2T_{ac}/m_a)^{1/2}$, e is the electron charge, Λ_a is the Coulomb logarithm, $Z_e=1$, $Z_i=1/2$ because ions do not scatter much off of electrons, ϕ_a is ϕ_e for electrons and ϕ_c for ions,

$$G(x) = \frac{\pi}{2}^{1/2}\ (1+\frac{1}{x})^{1/2}\ \ln\left[\frac{(1+\frac{1}{x})^{1/2}+1}{(1+\frac{1}{x})^{1/2}-1}\right] \qquad \text{(II.A.6)}$$

and $I(x) = 1 + x/2 - x^2/4$. The Logan-Rensink model is used for $(n\tau)_{ip}$ of ions in the plug.[5]

$$(n\tau)_{ip} = \left[\frac{\Lambda_{iip}\,(m_D/m_{ip})^{1/2}}{3.9\times10^{12}\ E_{inj}^{3/2}\ \log_{10} R_{eff}} + \frac{\Lambda_{eip}(m_H/m_{ip})}{10^{13}\ T_{ep}^{3/2}\ \ln (E_{inj}/E_{out})}\right]^{-1} \qquad \text{(II.A.7)}$$

where m_D is the mass of deuterium, m_H is the mass of hydrogen, m_{ip} is the plug ion mass, Λ_{iip} and Λ_{eip} are Coulomb logarithms, E_{inj} is the neutral beam injection energy, E_{out} is given by

$$E_{out} = \frac{E_{inj}}{1+\tau_i/\tau_{DR}} + \frac{(\phi_c+\phi_e)}{\left[\frac{R_p \sin^2\theta}{(1-\beta_p)^{1/2}} - 1\right]}\ \frac{\tau_i/\tau_{DR}}{(1+\tau_i/\tau_{DR})} \qquad \text{(II.A.8)}$$

where R_p is the plug mirror ratio; θ is the beam injection angle, taken here as $\pi/2$; β_p is the plug beta, and τ_i/τ_{DR}, the ratio of ion collision time to electron drag time, is given by

$$\frac{\tau_i}{\tau_{DR}} = .11 \left(\frac{E_{inj}}{T_{ep}}\right)^{3/2} \frac{\Lambda_{eip}}{\Lambda_{iip}} \frac{\log_{10} R_{eff}}{\ln(E_{inj}/E_{out})} \left(\frac{m_D}{m_{ip}}\right)^{1/2} \qquad \text{(II.A.9)}$$

where T_{ep} is the plug electron temperature and

$$R_{eff} = \frac{R_p/(1-\beta_p)^{1/2}}{1 + \frac{\phi_e+\phi_c}{E_{inj}}} \sin^2\theta \quad . \qquad \text{(II.A.10)}$$

For the potential ϕ_c, recognition is taken that the central cell ion temperature, T_{ic}, best characterizes a set of plasma parameters. Thus, ϕ_c is found by requiring $dT_{ic}/dt = 0$; this equation will be given later in the section.

T_{ep} can then be found from the equation for ϕ_c

$$\phi_c = \left(\frac{T_{ep}}{T_{ec}} - 1\right) \phi_b + T_{ep} \ln \left[\frac{n_p}{n_c} \left(\frac{T_{ec}}{T_{ep}}\right)^{\nu}\right] \quad . \qquad \text{(II.A.11)}$$

The case ν=0, which comes from assuming a Boltzmann relation between the barrier and the plug, is used for the parameters given in this report. Recent work by Cohen, which is still in progress, indicates that ν will be in the range 0.7 to 0.9.[6] This will probably require an increase in energy input to the plug - somewhat lowering Q values.

P_{eaux}, which is the auxiliary electron heating in the plug, is given by the requirement that dT_{ep}/dt=0; this is only relaxed if P_{eaux} is less than zero, in which case T_{ep} is allowed to vary and P_{eaux} is set to zero.

The plug electron power balance is given by

$$f_{ep} P_{eaux} + (n_p - n_{pass}) \nu^{ep/ip} (E_p - \frac{3}{2} T_{ep}) = \frac{3}{2} (n_p - n_{pass}) \nu^{ep/ec}$$
$$(T_{ep} - T_{ec}) + \frac{(n_p - n_{pass})^2}{(n\tau)_{ep}} (T_{ep} - T_{ec}) \qquad \text{(II.A.12)}$$

where f_{ep} is the fraction of auxiliary power which goes to the plug electrons; it has been assumed that the density of electrons trapped in the plug is $n_p - n_{pass}$, where flux conservation of electrons passing over the barrier ϕ_b is given by

$$n_{pass} = \frac{n_c}{B_{maxb}/B_p} \left[\frac{T_{ec}}{\pi(\phi_b + \phi_c)}\right]^{1/2} e^{-\phi_b/T_{ec}} \quad . \qquad \text{(II.A.13)}$$

E_p is the average plug ion energy; $\nu^{ep/ip}$ and $\nu^{ep/ec}$ are the collisional energy transfer rates between plug electrons and plug ions or central cell electrons; and $(n\tau)_{ep}$ is the Pastukhov loss rate for electrons from the plug to the central cell over the potential $\phi_b + \phi_c$.

The central cell electron power balance is given by

$$\frac{f_{ec}}{Rv} P_{eaux} + \frac{n_c^2}{4} \langle\sigma v\rangle_{DT} f_{e\alpha} E_\alpha \left(1 + \frac{E_R}{E_{fus}}\right) + \frac{3}{2} n_c \nu^{ec/ip} (T_{ip} - T_{ec})$$
$$+ \frac{3}{2} n_c \nu^{ec/ep} (T_{ep} - T_{ec}) + \frac{(n_p - n_{pass})^2}{R_v (n\tau)_{ep}} (T_{ep} - T_{ec})$$
$$= (\phi_e + T_{ec}) \left[\frac{n_c^2}{(n\tau)_{ec}} + \frac{n_c^2}{(n\tau)_{xfe}} + \frac{n_c^2}{2} \langle\sigma v\rangle_{DT}\right] + \frac{3}{2} n_c \nu^{ec/ic} (T_{ec} - T_{ic})$$
$$+ \frac{3}{2} \frac{n_c^2}{(n\tau)_{ic}} f_{is} T_{ec} + \frac{3}{2} J_{trap} \frac{2V_B}{V_c} T_{ec} \qquad \text{(II.A.14)}$$

where f_{ec} is the fraction of auxiliary power which goes to the passing electrons; R_v is the volume ratio $V_c/2V_p$; $f_{e\alpha}$ is the fraction of the alpha particle energy which goes to electrons, given by $f_{e\alpha}=.882 \exp(-T_{ec}/67.4)$;[7] E_α is the alpha particle energy; E_R is the average energy of the reacting ions, taken to be $E_R=45 + 1.5\ T_{ic}$;[2] and $\nu^{ec/ip}$, $\nu^{ec/ep}$, and $\nu^{ec/ic}$ are the collisional energy transfer rates between central cell electrons and plug ions, plug electrons, or central cell ions. The last term on the left-hand side is the power transferred by plug electrons being lost over the $\phi_b+\phi_c$ barrier, and being replaced by trapping of passing electrons. The first term on the right-hand side comes from theloss of electrons from the machine and the cold electrons which come in with the fueling ions; the third term comes from the cold electron current, if present; and the fourth term comes from cold electrons which come in with the ions required to replace ions removed from the barrier - this term will be absent if the ions from the barrier go into the central cell instead of escaping. The J_{trap} term helps depress T_{ec} and thus allows higher n_c for a given β_c, but is not included for the case used in this report.

The plug ion power balance is given by

$$\frac{n_p^2}{(n\tau)_{ip}} E_{inj} = \frac{n_p^2}{(n\tau)_{ip}} \frac{\langle\sigma v\rangle_{cxp}}{\langle\sigma v\rangle_{ionp}} (E_p - E_{inj}) + \frac{n_p^2}{(n\tau)_{ip}} E_{out} + n_p \nu^{ip/ep} (E_p - \tfrac{3}{2} T_{ep}) + n_p \nu^{ip/ec} (E_p - \tfrac{3}{2} T_{ec}) \quad \text{(II.A.15)}$$

where $\langle\sigma v\rangle_{cxp}$ is the plug charge exchange rate, $\langle\sigma v\rangle_{ionp}$ is the plug ionization rate, $\nu^{ip/ep}$ and $\nu^{ip/ec}$ are the collisional energy transfer rates between the plug ions and plug electrons or passing central cell electrons. The term on the left-hand side is the power deposited by neutral beams. The first term on the right-hand side is the energy lost to charge exchange, and the second term is energy lost by particles escaping from the plug.

The central cell ion power balance is given by

$$\frac{n_c^2}{4}\langle\sigma v\rangle_{DT}\left[f_{i\alpha}E_\alpha\left(1+\frac{E_R}{E_{fus}}\right)-E_R\right]=\frac{3}{2}n_c\nu^{ic/ec}(T_{ic}-T_{ec})+(\phi_c+T_{ic})$$

$$\frac{n_c^2}{(n\tau)_{ic}}+T_{ic}\frac{n_c^2}{(n\tau)_{xfi}}+\frac{3}{2}T_{ic}\left[\frac{n_c^2}{(n\tau)_{ic}}+\frac{n_c^2}{(n\tau)_{xfi}}+\frac{n_c^2}{2}\langle\sigma v\rangle_{DT}\right]\frac{\langle\sigma v\rangle_{cxc}}{\langle\sigma v\rangle_{ionc}} \qquad \text{(II.A.16)}$$

where $f_{i\alpha} = 1 - .908\exp(-T_{ec}/101.7)$ is the fraction of alpha particle energy deposited in the ions;[7] $\nu^{ic/ec}$ is the collisional energy transfer rate between central cell ions and central cell electrons; $\langle\sigma v\rangle_{cxc}$ is the central cell charge exchange rate; $\langle\sigma v\rangle_{ionc}$ is the central cell ionization rate; and $(n\tau)_{xfi}$ is the cross-field $(n\tau)$. Note that most particles reflect off of B_{maxb}, where the field is circular; they do not see the quadrupole fields and radial transport should be small for both ions and electrons - it is neglected here.

When all of the power balance equations have been satisfied, Q is computed from

$$Q = \frac{P_{fus}V_c}{(P_{NB}+P_{eaux})2V_p+P_{pump}2V_B} \qquad \text{(II.A.17)}$$

where P_{NB} is the neutral beam power per unit volume into the plasma, P_{eaux} is the auxiliary heating of the plug plasma, and P_{pump} is the power required to replace ions lost from the barrier, $P_{pump}=J_{trap}(\phi_b+T_{ic})$.

Although the technical problem of achieving a high barrier mirror ratio in a relatively short length must be overcome, and the central cell beta limit must be found, the Q=33 with reasonable parameters found from this analysis is encouraging. In particular, leeway exists which will allow the relaxation of troublesome restrictions should they appear.

References

1. K. Shaing, R. Conn, J. Kesner, University of Wisconsin Report UWFDM-267 (Oct. 1978) and Bull. APS 23, 882 (1978).

2. G. Carlson, et al., University of California Lawrence Livermore Laboratory Report UCRL-52836 (Sept. 1979).

3. V. Pastukhov, Nucl. Fus. 14, 3 (1974).

4. R. Cohen, M. Rensink, T. Cutter, and A. Mirin, Nucl. Fus. 18, 1229 (1978).

5. B.G. Logan and M.E. Rensink, University of California Lawrence Livermore Laboratory, MFE Memo MFE/CPI/78-181.

6. R. Cohen, University of California Lawrence Livermore Laboratory MFE Memo MFE/TC/79-130 and private communication.

7. D. Baldwin, B.G. Logan, and T.K. Fowler, University of California Lawrence Livermore Laboratory Report UCID-18156, and M. Rensink, private communication.

II-B. RF Heating Roles in the Tandem Mirror Reactor

We have considered the problems of electron heating in the end plugs of the University of Wisconsin Tandem Mirror Reactor. This provides an attractive method for reducing the plug density, neutral beam injection energy and power requirements as well as enhancing the ambipolar potential with the addition of the thermal barrier.

We have concentrated on the use of Electron Cyclotron Range of Frequencies (ECRF) and are formulating the ray tracing problem for heating the end cell. We have also briefly considered the possible roles of the ICRF regime for supplementary ion heating in the end plug if it is needed and whether with its improved efficiency it could provide the electron heating in the end plug.

Electron Cyclotron Heating of the Plug

Radiofrequency heating of the plug electrons plays a major role in the success of the recent implementation of a thermal barrier in the standard tandem mirror reactor. A high plug electron temperature ($T_{ep} \sim 200$ keV) is designed to raise the central cell ion confining potential ϕ_c and to lower the plug density so that neutral beam and magnet technological requirements in the plug will be eased. Among various candidates, electron cyclotron resonant heating (ECRH) stands out because of its near-100% absorption efficiency and the projected availability of high-power gyrotron tubes in the gigahertz frequency range.

For the preliminary UW-TMR design parameters, the electron heating zone is located in the transition region between the end-plug and the thermal barrier. For a local magnetic field of 2 Tesla, the wave frequency is 56 GHz and the

total power (for both plugs) absorbed by the electrons is 25 MW. Assuming a 100% electron absorption efficiency and a 40% gyrotron efficiency, the input electron power is at least 62.5 MW. In this note, we will present some preliminary findings concerning several key aspects of the ECRH system design and describe the ongoing work in these areas.

Finite-β Effects

In the preliminary UW-TMR design, the plug β_p is 0.64 and the central cell β_c is 0.5. Besides playing an important part in the plasma stability problem, the plasma β modifies the local magnetic field from its vacuum value and thus will change the wave accessibility and propagation picture. Thus, an accurate spatial profile of the plasma β and the magnetic field is needed before a ray tracing analysis of ECRH in the plug can be carried out. We are presently modifying an existing code, written by Friedland, Bernstein and Porkolab to incorporate the effects of finite β in the ray tracing analysis.

Relativistic Effects

A plug electron temperature of 200 keV requires that the electrons be treated relativistically. Its effect on wave dispersion and local absorption calculations as opposed to the low-β situation in TMX will be carefully considered. Problems such as mode selection (either ordinary or extraordinary mode or both), field polarization modification along the ray trajectory and the resonance width will be examined. Inclusion of relativistic effects considerably complicates the hot plasma dispersion relation in that the velocity integrals in $v_\perp$ and $v_\parallel$ are not coupled and need to be evaluated numerically.

Wave Injection

Because of the short wavelengths in the relevant frequency range, the microwave energy can be transmitted in narrow beams, providing considerable flexibility in the coupler design. The high power involved necessitates an array of beams incident on the plasma. The modified ray tracing code can be used to find the optimum beam array for maximum absorption and engineering compatibility. In particular, the angles of incidence and wave spectrum for this optimum array will be examined.

Improved ECRH Transmission System

For our design analysis, we are considering techniques for converting the TE_{02} gyrotron polarization to a linear polarization suitable for transmission in a very low-loss beam-waveguide system with metalized mirrors and/or dielectric "lenses". This would have the advantages of transmitting a linear polarization which could be absorbed in a single pass and minimize the neutron problem and losses along a conventional overmoded circular waveguide transmission system. All mirrors or lenses other than the last one could be shielded from the neutron flux. The last mirror could also be used to focus the rays in the desired region of the mirror plug. Several systems (and possibly frequencies) would be required to couple the 25 MW of supplementary power to the plugs.

II-C. Passive Thermal Barrier

The thermal barrier concept[1] interposes a negative electrostatic potential between the central cell and plug of a tandem mirror. This is accomplished by adding a mirror cell between the central cell and the plug and can only be maintained if a means is found for preventing positively charged ions from trapping in this region and filling it.

We have proposed that this be accomplished by a magnetic geometry such that ions that trap in the cell will drift out to a limiter.[2] This is done by taking advantage of the ellipticity of the flux tube leaving a quadrupole plug and employing an elliptic cross-section barrier cell which does not become recircularized until the central cell side mirror throat (Fig. II-2). (The ellipticity of the flux tube leaving the plug is typically 30:1.) The grad-B drift ($V_{\nabla B}$) will tend to drift trapped ions and electrons out from this flux tube and these ions could then be removed by limiters or charge exchange on neutral gas.

High-Z impurities, which are more collisional than hydrogen, will tend to trap faster in the barrier cell and therefore drift pumping provides a method of purifying the central cell. (A tandem mirror without a barrier cell is particularly susceptable to impurity buildup since high-Z ions are better confined than hydrogen in an electrostatic well.) The loss rate, L, of these ions would be approximately given by the pitch angle scattering time reduced because of the small barrier to central cell volume ratio and because of the density dips in this region:

$$L \sim \frac{n_Z(b)\, n_H(b)}{\frac{(n\tau)_Z}{R_b}} \frac{2V_B}{2V_B+V_C} \qquad \text{(II-C-1)}$$

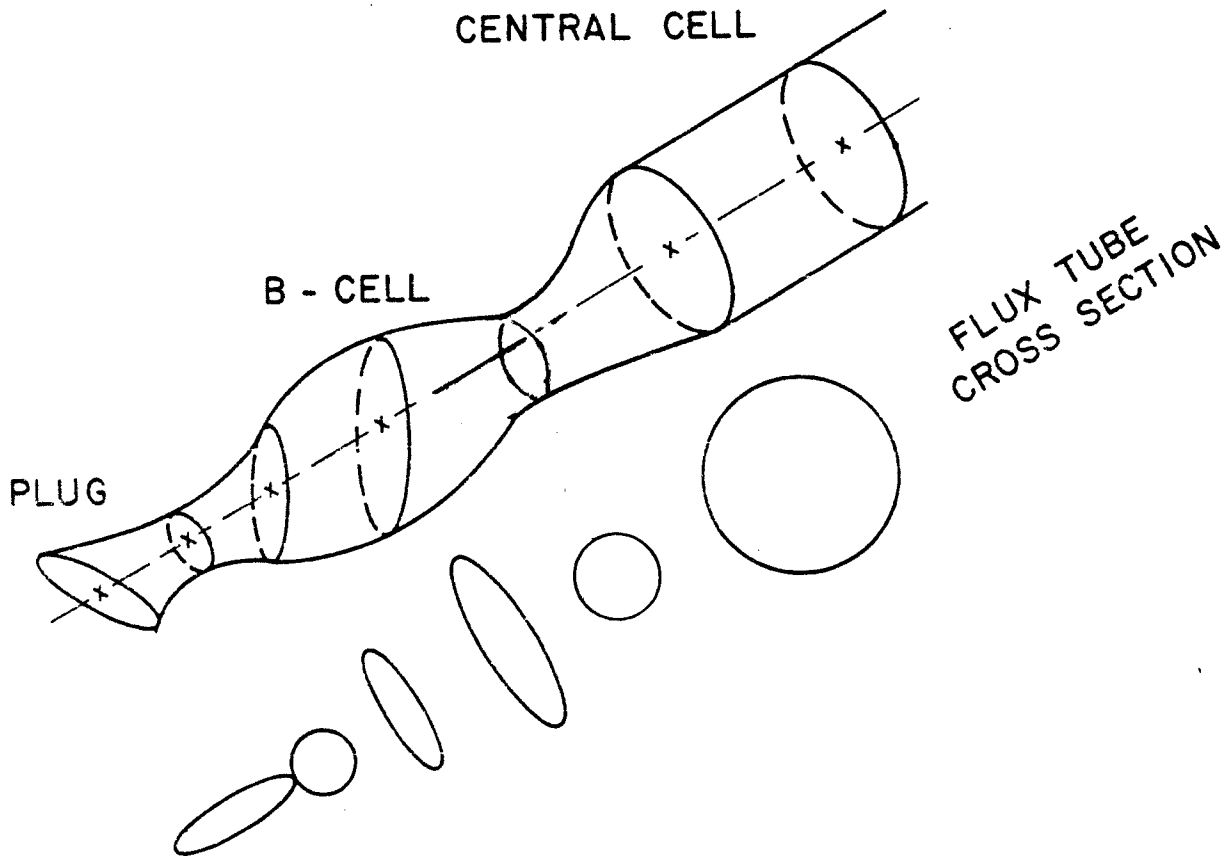

Figure II-2. Schematic of Passive Thermal Barrier Concept.

where $(n\tau)_Z$ is the 90° scattering time for ions of charge Z, and the hydrogenic and high Z densities, n_H, n_Z are evaluated within the barrier cell. Considering the mass (A) and charge (Z) dependence of $n_Z^{(1,2)}$ and $(n\tau)_A$ indicates $L \propto Z^{3/2}/A^{1/2} \sim Z$. For the volume and mirror ratios of our base case reactor we get a barrier $n\tau$ of $n\tau_b \approx 7.5 \times 10^{14}\ A^{1/2}/Z^{3/2}$. This will then yield $n\tau_b = 1.2 \times 10^{15}$ for D-T (A=2.5), while for an impurity such as iron $n\tau_b = 5.2 \times 10^{13}$.

One question of potentially serious import is the E x B particle drift that results from the radial potential of the central cell, which causes ion drifts along the elliptic flux tube. A comparison of the E x B drift (V_E) with the grad-B drift gives

$$\frac{V_{\nabla B}}{V_E} = \frac{2\varepsilon_{\parallel}+\varepsilon_{\perp}}{e\delta\phi}\left(\frac{\ell_\phi}{\rho}\right) \qquad \text{(II-C-2)}$$

for ℓ_ϕ the characteristic potential length ($E \sim \frac{\delta\phi}{\ell_\phi}$), $\varepsilon_{\perp(\parallel)}$ the perpendicular (parallel) ion energy and ρ the magnetic field radius of curvature. If the barrier cell mirror has a parabolic dependence near the midplane of the form

$$B = B_0(1+(R-1)Z^2/L_B^2) \qquad \text{(II-C-3)}$$

with R the mirror ratio, and L the characteristic length, we can find the midplane radius of curvature ρ to be

$$\rho = \frac{L_B^2}{2r(R-1)} \qquad \text{(II-C-4)}$$

for r the midplane radial position. We can then write the drift velocity ratio as

$$\frac{V_{\nabla B}}{V_E} = \left(\frac{2\varepsilon_{\parallel}+\varepsilon_{\perp}}{e\delta\phi}\right)\frac{2r\ell_\phi(R-1)}{L_B^2} \quad . \qquad \text{(II-C-5)}$$

The mirror ratio from two loops of radius a_b and separation $2L_B$ is approximately $R_b \approx \frac{1}{2}(1+L_B^2/a_b^2)^{3/2}$. Furthermore, for an ellipse of ellipticity ε ($\varepsilon = r_{max}/r_{min}$) with r_{max} (r_{min}) the large (small) radius of the ellipse at the barrier midplane would have a circular cross-section at the central cell side mirror throat of radius r_m given by $r_m = r_{min}\sqrt{\varepsilon/R_B}$. If $\ell_\phi \sim r_{min}$ Eq. (II-C-5) becomes

$$\frac{V_{\nabla B}}{V_E} = \left(\frac{2\varepsilon_{\parallel}+\varepsilon_{\perp}}{\delta\phi}\right)\left(\frac{2r_m}{a_b}\right)\frac{r}{a_b\sqrt{\varepsilon}}\frac{\sqrt{R_b}(R_b-1)}{(2R_b)^{2/3}-1} \quad .$$

Clearly the grad-B drift becomes less important at small radius, small mirror ratio, low energy or large radial electric fields. For relatively small radial electric fields passive pumping could pump most of the cell although the region of the ellipse near the axis would still require an auxiliary pump mechanism (this would be true even with no radial potential because the circular drift of ions at small radius would stay within the ellipse).

We are presently pursuing drift orbit calculations to study the efficiency of the passive pumping scheme and to evaluate the amount of power needed for additional pumping.

References

1. D.E. Baldwin and B.G. Logan, to be published in Phys. Rev. Lett. (1979). Also Lawrence Livermore Laboratory UCID-18156 (1979).

2. J. Kesner, to be published in Comments on Plasma Physics and Thermonuclear Fusion (1979). Also University of Wisconsin Report UWFDM-303 (1979).

III. Tandem Mirror Magnet Design

III-A. General Comments

The magnetic field requirements of a Tandem Mirror Reactor are (i) a set of central cell solenoidal magnets of fairly straightforward design and (ii) end plugs of complex design. So far as the magnet design is concerned, the crucial problems lie in the end plugs and our principal efforts have been with them. In the first period of our TMR study (up to about April, 1979), our magnetic field design followed that of a classical TMR without thermal barriers. The end plug contained a very high field (14.5 Tesla), high stress Yin Yang and solenoid pair. Here we summarize the features of the design of this end plug. A fuller account is being prepared for presentation at the Fusion Engineering Conference[1].

The fluid situation with respect to the plasma physics of the TMR has meant that we have not yet achieved a consistent design for an end plug with thermal barriers because the magnetic field requirements of the end plug are still in question. At the time of writing (end of October), it appears that the end plug might contain 2 Yin Yangs of lower field ($\sim$6 Tesla in the throat) or follow the design shown in Figures III-1 and III-2, where the high field is now transferred to a solenoid (B_{max} = 15.5T) and the C coil and Yin Yangs have peak fields less than 10T. We anticipate reporting on this design in more detail at the November review. At the present time, it appears as if the field requirements can be met with reasonable values of J_c (2000 A/cm^2 in the barrier solenoid, 2500 A/cm^2 in the remaining coils) and the modified end plug appears to compare favorably with our initial classical TMR design.

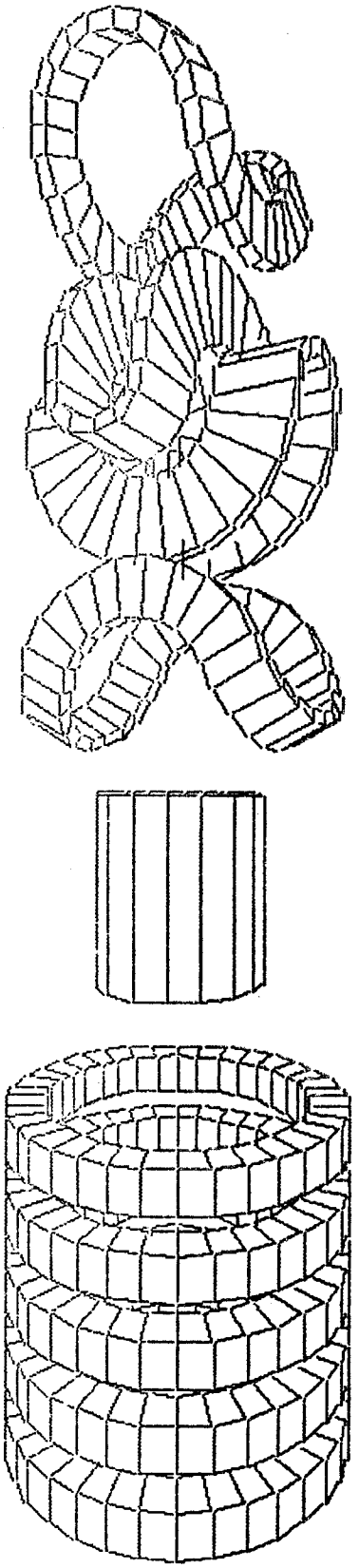

Figure III-1 General Design of TMR End Plug With Thermal Barrier

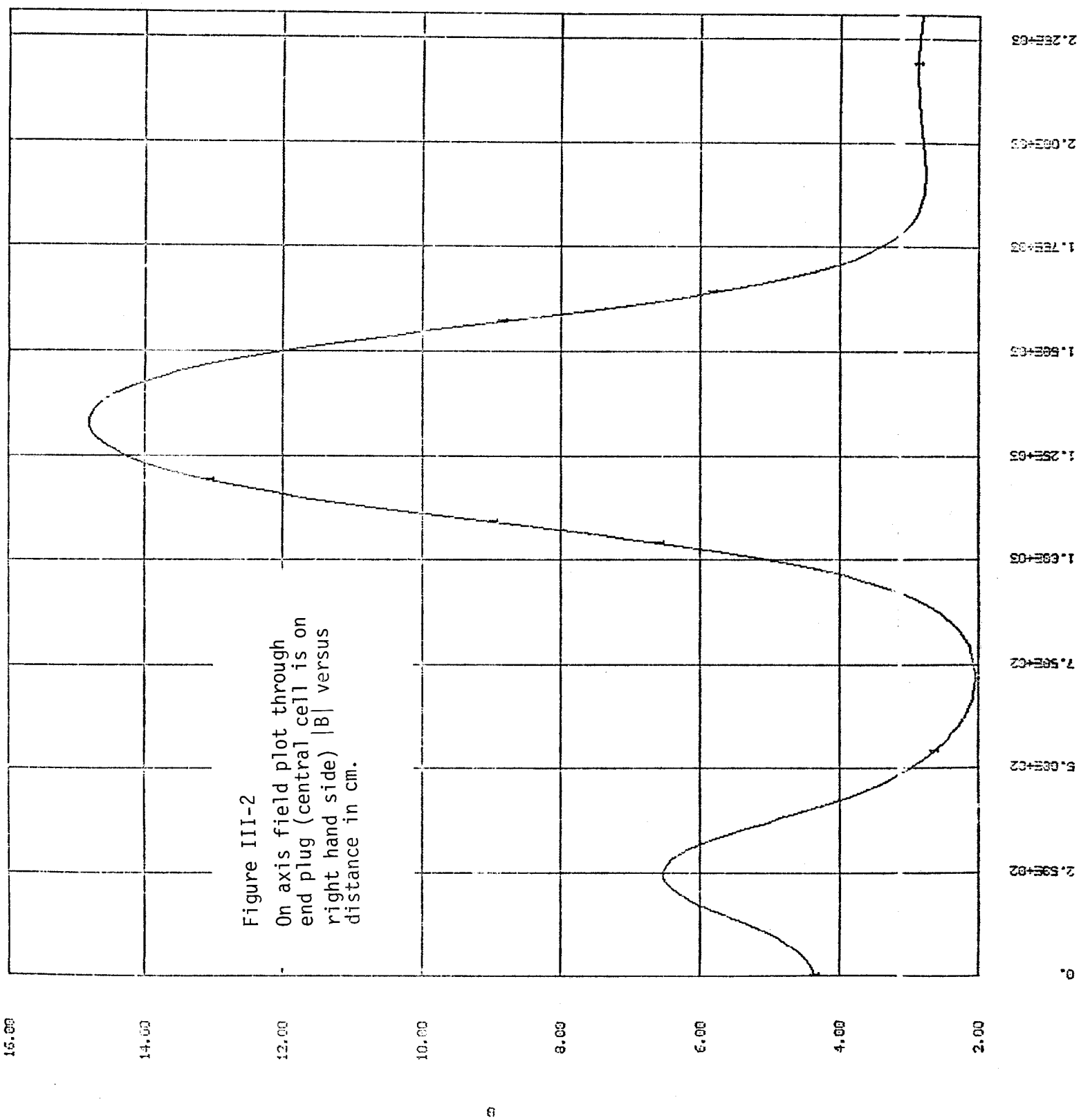

Figure III-2

On axis field plot through end plug (central cell is on right hand side) |B| versus distance in cm.

III-B. End Plug Design

The design of the end plug went through many iterations. The main features of the final design are summarized in the Table below and in Figure III-3.

	Design Goals	Final Design
Maximum field in mirror throat	$\geq$ 10 T	(11.0)
Maximum field at conductor	$\leq$ 15T	(14.45)
Mirror ratio	$\geq$ 1.1	(1.14)
Mirror length	$\leq$ 4.5 m	(4.1)
Radial well depth	$\geq$ 4%	(4%)
Blanket and shield thickness	$\geq$ 70 cm	(80)
Beam port aperture	$\sim$ 80 cm	(80)
Current density in Yin Yang	$\leq$ 1800 A/cm^2	(1800)
Yin Yang current	$\leq$ 20 MA	(20.81)

It was clear at the outset that a credible design of a 15-17 T Yin Yang would be difficult in view of the high fields, high stresses and unfavorable cooling arrangements of the Yin Yang. Since the plasma physics appeared to require the base parameters listed in the Table, thus dictating the high field Yin Yang, we concentrated our design effort in this area. The design chosen was the Yin Yang and split solenoid pair illustrated in Fig. III-3. Of the central field of 9.6T, 4.6T is supplied by the Yin Yang.

The principal design problem in our view is the very high stress ($\sim$ 20 ksi average) transverse to the conductor and the problems of conductor crushing, cooling channel integrity and large intra- and

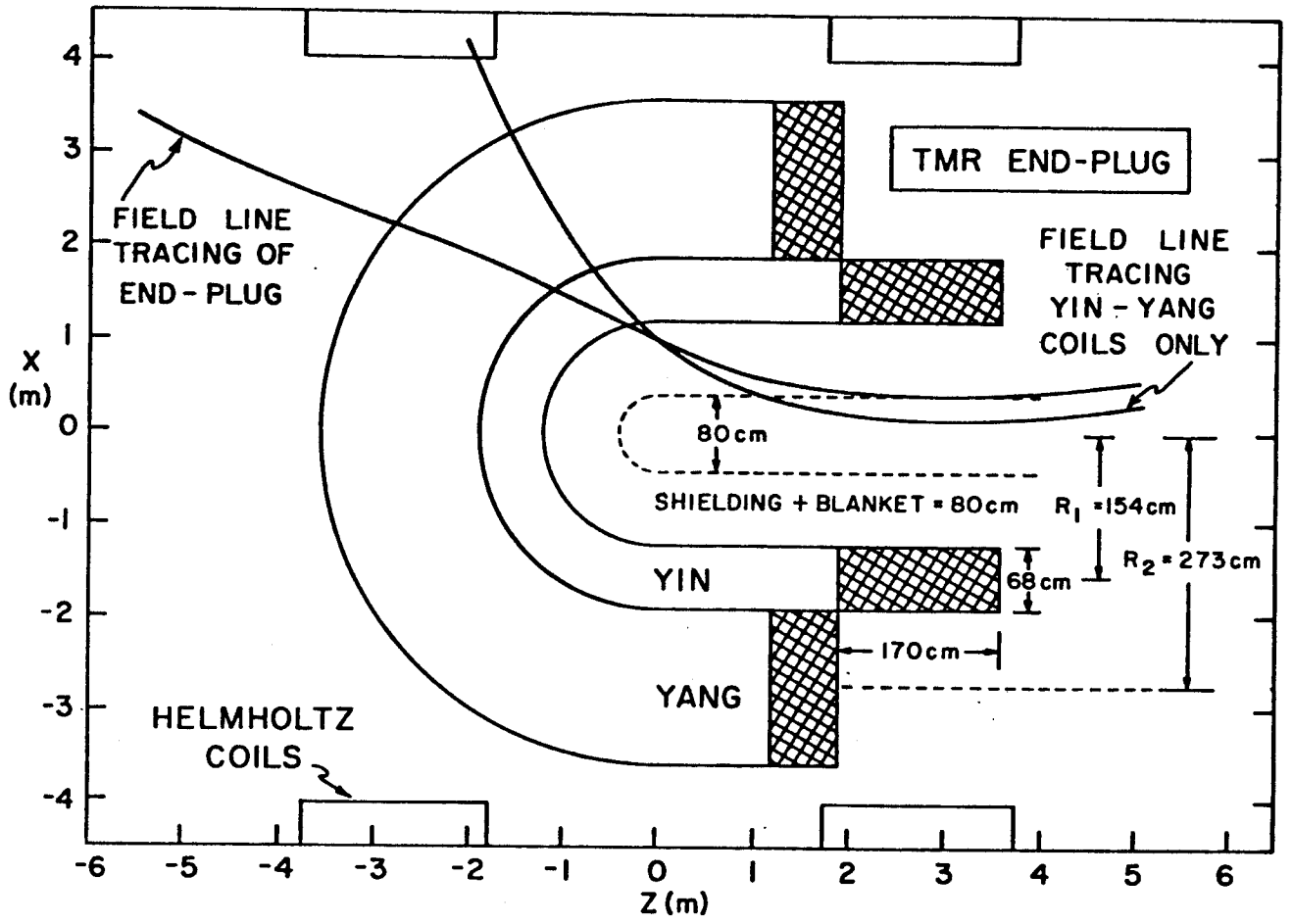

Figure III-3 Classical TMR End Plug

inter-coil forces.

The magnetic loads on the Yin Yang were orginally computed from EFFI and a structural analysis of the forces external to the conductor bundle were made by Irving Ojalvo of Grumman. The in-plane and out-of-plane loads from this analysis are given in Fig. III-4. The magnetic loads, which are very large, are allowed to accumulate to a coil case 20 cm thick, operating at 80 ksi. Stiffening members connect the sides of each coil to itself and one coil to another. Adequate space is available for beam injection. Although accumulating the magnetic loads to the coil case eases the coil construction it does impose large average stresses of ∿20 ksi on the conductor. Since the stresses are transverse to the conductor axis no credit was taken for conductor strength in designing the coil case.

The high field in the Yin Yang coil (14.5T) dictates the use of Nb_3Sn. Due to the high field, the available J_c can be increased by 50% on reducing the temperature from 4.2 to 1.8K. Permitted strains in the Nb_3Sn were set at 0.3% in bending and 0.5% in tension.[2,3]

The high transverse stress poses a number of problems for the integrity of cooling channels and in addition dictates that such channels should be as small as possible so as to reduce bearing stresses. A Yin Yang conductor sees all orientations to the vertical, giving rise to concern over vapor locking when He I at 4.2 K is used as coolant. For these combined reasons, we found that we could not design a credible He I 4.2 K cooled conductor with an overall block J_c of better than 1500 A/mm^2. He II cooling at 1 atmosphere pressure does allow 1800 A/cm^2 at 14.5T to be achieved due to the higher permissible heat flux and the increased J_c in the Nb_3Sn. Since cooling is now by conduction rather than convection and bubble transport, there is no danger of vapor locking for the fluxes chosen[4].

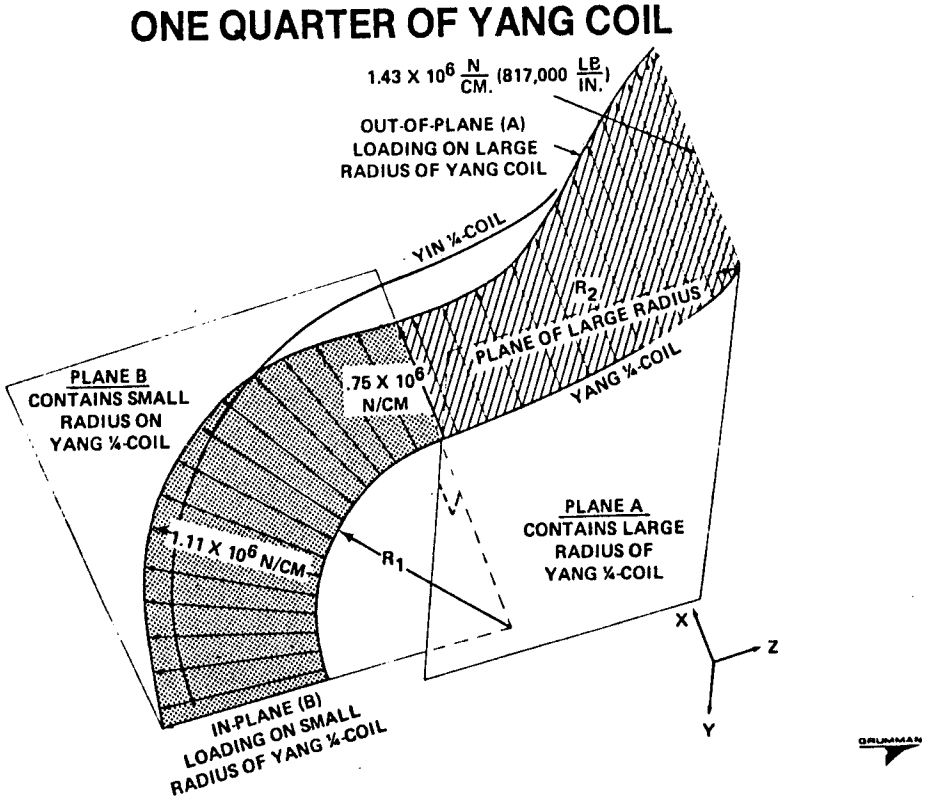

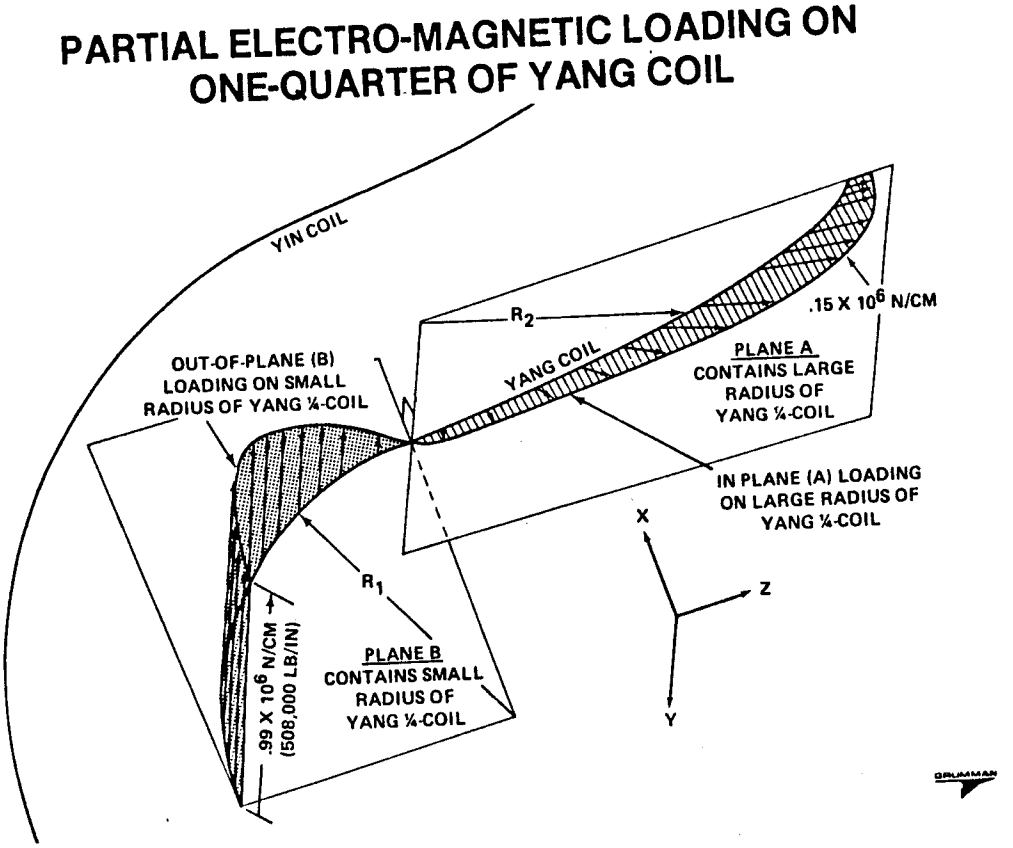

Figure III-4 In plane and out of plane loads on one quadrant of Yang coil.

Operation at 1 atmosphere in He II is dictated by the voltage breakdown margin of the liquid (proportional to fluid density[5]). Since the TMR is operated in DC mode, most sources of heat can be intercepted at 4.2 K and the additional cost of the 4.2 K to 1.8 K refrigeration is small.

At high fields Al appears to have a number of advantages over Cu as a stabilizer (viz lower ρ and lower magnetoresitivity). However, in the case of the TMR Yin Yang, Al does not appear to be very attractive since its very low yield strength demands that separate structural members be placed around the conductor to support the transverse loads. Al also offers some compatibility problems with Nb_3Sn in view of its low M.P. (660°C). Copper in the 3/4 hard condition [6] or strengthened with an in situ dispersion of Nb[7] offers a combination of strength and conductivity which permits additional structural elements to be avoided.

Our preferred conductor design for the Yin Yang is tabulated in Table III-1 and shown in Fig. III-5. It can be seen that its design is particularly simple. He II cooling permits the surface heat flux to be 0.5 W/cm^2 and all cooling can be performed on the outside faces. No separate conductor structure is needed since 3/4 hard OFHC Cu has a yield strength of 39 ksi for ρ (H=0) = 2.9×10^{-10} Ω m[6]. The conductor surface is 50% obscured by G10 insulator and follows the MFTF design (slotted sheets for layer to layer insulation and buttons for turn to turn). Recent tests at MIT indicate that G10 will accept up to 60 ksi in compression.[8]

III-C. Central Cell Magnets

A series of scaling relations have been developed for the central cell magnets having a central field of 2 Tesla. Detailed design of these magnets awaits a final decision on radius and plasma

Table III-1

DESIGN OF COPPER CONDUCTOR

Operating current		5000 A
Operating current density in Nb_3Sn (bronze + Nb)		200 A/mm^2
Critical current density at 1.8 K/14.5 T		330 A/mm^2
Overall winding current density		18 A/mm^2
Compressive stress in conductor		25000 psi
Yield strength of 3/4 hard Cu		39000 psi
Electrical resistivity at 14.5 T with 10^6 dpa		1.1×10^{-7} Ωcm
Volume fractions:	Cu stabilizer	64%
	Nb_3Sn + bronze	9%
	Helium	13.5%
	Insulator	13.5%
Heat generation/cm		1.44 W/cm
Heat flux from conductor surface*		0.5 W/cm^2
Heat flux through cooling channel		1.44 W/cm^2
Critical heat transfer length		≃1 m

*50% surface coverage by insulator on both faces.

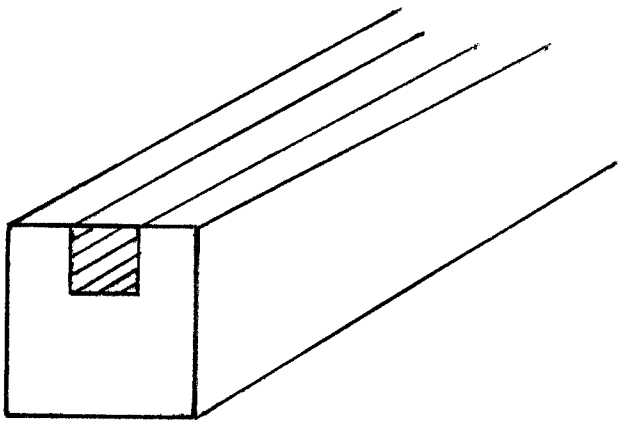

Figure III-5: Yin Yang Nb_3Sn conductor. Stabilizer is 3/4 hard Cu; bronze + Nb_3Sn conductor is shaded. Conductor is 50% covered by insulation and cooled with He II.

parameters (eg. maximum permissible field ripple). The general design parameters and scaling relations are shown in Table III-2.

REFERENCES

1. S.O. Hong, D.C. Larbalestier, L.P. Mai, I.N. Sviatoslavsky, I. Ojalvo to be given at 8th Fusion Engineering Conference.

2. S.O. Hong, D.C. Larbalestier, IEEE Tans. MAG 15 784 (1979).

3. D.W. Deis, D.N. Cornish, D.G. Hirzel, A.R. Rosdahl, Proc. of 7th Symp. on Engineering Problems of Fusion Research, p. 1263 (1977).

4. S.W. Van Sciver,, Proc. of 7th Symp. on Engineering Problems of Fusion Research, p. 690 (1977).

5. K.F. Hwang, S.O. Hong, Proc. of 7th Symp. on Engineering Problems of Fusion Research, p. 1531 (1977).

6. P.T. Clee, Engineering Design Note 001 Rutherford Laboratory.

7. J. Bevk, J.P. Harbison, J.L. Bell JAP 49 6031 (1978).

8. H. Becker, MIT National Magnet Lab, private communication.

Table III-2

Central Cell Magnet Details

Al Stabilizer	RRR = 1000
NbTi Superconductor	$J_c = 4 \times 10^5$ A/cm^2
Al Alloy Structure	σ = 30 ksi
Block J_c	= 4000 A/cm^2
Central Field	= 2 Tesla

Scaling Relations

Wt. of Nb-Ti	9 RL (kg)
Wt. of Al Stabilizer	500 RL (kg)
Wt. of Al Alloy Structure	70 R^2L (kg)
Wt. of Al Alloy Dewar	480 $L/\Delta L^{1/2}$ (kg)

L = length of central cell (m)

ΔL = separation between magnets (m)

R = magnet radius (m)

IV. Tandem Mirror Blanket Design

IV-A. Design Philosophy

The TMR design philosophy is to use the experience obtained from the recent studies on magnetically confined D-T Tokamak reactors, combine it with the unique features of the tandem mirror to obtain an attractive design of a TM power reactor. It is aimed at maximizing the strengths of the tandem mirror while mitigating its weaknesses. The end product should be a safe, reliable, maintainable and a relatively economic power reactor. We believe that the blanket design described here is consistent with this philosophy.

The unique safety problems associated with a DT fusion reactor blanket are mostly related to tritium breeding. The chemical reaction of lithium or lithium bearing compounds with water, and tritium confinement are the primary areas of concern. Such a system can be designed to either minimize the possibility of an accident or else minimize the consequences of an accident. The second approach results in a simpler system and has, therefore, been adopted here. In order to minimize the consequences of an accident, the breeding material must be relatively inert toward water and should have a low tritium solubility. Hence $Li_{17}Pb_{83}$ has been selected for this purpose.

Early design studies have attempted to utilize high temperature and advanced technology to obtain higher efficiency thermal cycles and thus minimize environmental impact. However, it was soon realized, particularly for tokamaks, that high temperature systems present severe problems, especially in the areas of tritium confinement and radiation damage. It also became apparent that higher efficiency does not always translate into better economics. In the TMR design we have chosen a moderate temperature

for the blanket and a high pressure steam cycle for the power conversion system. We believe this results in a reliable and economically attractive reactor.

Perhaps the most attractive feature of the TMR is the simplicity of the central cell. The design philosophy has been to take full advantage of this basic cylindrical geometry to come up with a blanket which is simple to fabricate, lends itself easily to mass production and can be realistically maintained by remote control.

IV-B. Blanket Materials

1) Breeding and Cooling Material

The criteria for the selection of a suitable breeding and cooling material are:

1 - Breeding ratio $\geq$ 1.1,

2 - Material and structural compatibility,

3 - Relative inertness with respect to water, thus impacting on safety,

4 - Consistent with a low tritium inventory, good tritium containment and ease of recovery,

5 - Simplicity and reliability of blanket design.

Although the goal is to satisfy all these requirements at the same time, realistically it is very difficult. We have attempted to satisfy as many of these criteria as possible.

A breeding ratio of $\geq$ 1.05 is an absolute necessity in a pure D-T fusion reactor. Pure lithium, Li_2O and LiPb (in various atomic proportions) are the only materials which can achieve such a breeding ratio in a realistic blanket without neutron multipliers. In this design we have chosen $Li_{17}Pb_{83}$ as the breeding/cooling material primarily for its relative inertness to

water and its low tritium solubility. The chemical inertness comes from the low lithium activity and the large thermal sink provided by the lead. The low tritium solubility reduces the blanket tritium inventory and thus minimizes the effects of a tritium release accident. However, the resulting high tritium partial pressure makes its containment more difficult and the low inventory causes a problem in tritium recovery.

It is obviously advantageous to choose a breeding material which can also be the coolant. Such a choice results in a simpler design and mitigates the problems of heat transfer. Natural lithium has been considered in many early designs of fusion reactors, however, it has problems with MHD effects and safety considerations. The relatively low and uniform magnetic field in the TMR central cell not only reduces the MHD effects, but can be used to an advantage for flow distribution. Because of its low activity relative to water, $Li_{17}Pb_{83}$ has a considerable margin of safety over lithium. It should also be pointed out, that because of the very low thermal loading on a TMR first wall, a common cooling/breeding material selection results in a blanket with no major heat transfer surfaces. This considerably reduces the thermal stress on the structure and could result in a longer wall life.

The selection of $Li_{17}Pb_{83}$ as the cooling/breeding material satisfies all the indicated criteria except two, namely good tritium containment and recovery. These two problems will need further investigation.

2) Structural Material (HT-9)

The material chosen for the first wall for coolant tubing and supports throughout the blanket is ferritic (or martensitic) steel containing 8 to 12% Cr. The prime reason for this is its high resistance to void formation.[1] Swelling in this material under fast neutron irradiation is at least one

order of magnitude lower than 316 stainless steel (cold-worked), for irradiation > 1 x 10^{23} n/cm^2 (E > 0.1 MeV). In addition the ferritic steels show improved in-reactor creep resistance over 316 SS up to ~600°C. As a consequence the ferritic steels, when optimized for composition, offer the possiblity of a substantial increase in lifetime over 316. However it has not yet been shown that the favorable radiation resistance will be retained under 14 MeV neutron irradiation with much higher helium and hydrogen production rates.

The simple geometry of the tandem mirror central cell is an advantage in that the number of welds can be greatly reduced by using shaped, seamless tubes. However the ferritic steels will require post weld heat treatment for any welds that are needed and in our design such welds can be treated in the assembly factory before sending the unit to the field.

3) Material Compatibility

Since lead corrodes the iron base alloys more severely than the alkali metals, experience with liquid lead is the best indication of corrosion of HT-9. Iron is more resistant than its alloys since both chromium and particularly nickel dissolve more readily in liquid lead. The 8-12 Cr (HT-9) steels are therefore more resistant than 316 stainless steel, for example.[2]

The rate of dissolution attack is slow at temperatures below 600°C and can be reduced to negligible proportions by inhibition of the lead with 250 ppm of zirconium or titanium.[2]

The principal effect of the lithium is expected to be a possible decarburization. However, the iron base alloys do not differ greatly in C content and the reduced lithium activity in this case should essentially eliminate this difficulty. Mass transfer is not expected to be a problem at these temperatures particularly since the same ferritic alloy will be used throughout the coolant cycle.

IV-C. Neutronic Analysis

In this section we present the neutronic design for the TMR central cell blanket and shield. The general neutronic design goals for the blanket and shield are as follows:

- Tritium breeding ratio greater than 1.1
- Energy recovery greater than 99 percent
- Low inventory of radioactive material
- Maximum resistivity change in superconductor stabilizer less than 50%
- Maximum critical density change in the superconductor less than 2%
- Tolerable lifetime radiation dose in the superconducting magnet insulators.

The blanket and shield discussed in this section meets these criteria, however it does not represent an optimized design.

The neutronic and photonic calculations were made with the one dimensional transport code ANISN. A P_3-S_8 approximation in cylindrical geometry was utilized.

The transport cross sections used were a coupled 25 neutron-21 gamma group data library created from the RSIC DLC-41B/Vitamin C Data Library. Kerma factors, helium and hydrogen production cross sections, and displacement cross sections were created from the DLC-60/MACLIB-IV Data Library. Both the DLC-41B and DLC-60 Libraries were produced from ENDF/B-IV files. A standard CTR weighting function was used to collapse the DLC-60 and DLC-41B libraries into 25 neutron and 21 gamma energy groups.

A schematic of the blanket is shown in Figure IV-1.

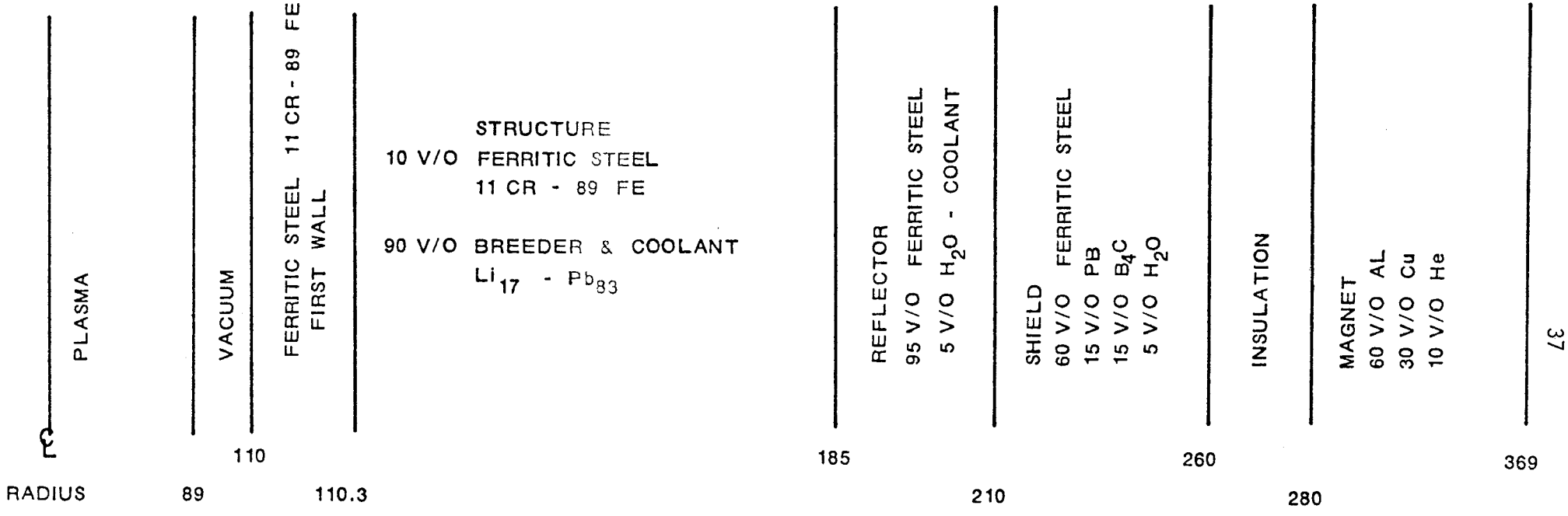

FIG. IV - 1 BLANKET SCHEMATIC

The choice of $Li_{17}Pb_{83}$ as coolant and breeder material is discussed elsewhere in this section. A 10 volume percent structure was used as it was expected that this amount would be an upper limit of material required. Also, earlier calculations have shown that a breeding ratio of 1.1 could be obtained with this amount of structure and a 75 cm thick blanket. A 25 cm ferritic steel, water cooled reflector is used. This reflector will run hot and the energy in it will be recovered. The shield is based on models from previous studies.

For each 14.1 MeV neutron generated in the plasma, 18.9 MeV of energy is deposited in the blanket which is an energy multiplication of 1.33. Of the energy deposited, 7.6 MeV is from neutron and charged particle reactions and 11.3 MeV from gamma interactions. About 10% of the energy is deposited in the reflector and less than 1% in the shield.

For 1 MW/m^2 wall loading the average power density in the breeding blanket and reflector is .92 W/cm^2 or 92 MW/m of central cell.

The tritium breeding ratio is 1.107 with about 2% from the $Li^7(n,n\alpha)T$ reaction.

In the magnets, the heat deposited from neutron and gamma interactions is $.87 \times 10^{-7}$ W/cm^3 and a maximum of 6×10^{-6} dpa/yr in the copper stabilizer. Both of these figures are based on a 1 MW/m^2 wall loading and are within the design limits. Lead plays the dominant role in determining the neutronic performance of the blanket. Lead has high n,2n and n,3n cross sections which increase the neutronic performance through neutron multiplication. The extra neutrons increase the atomic displacements as well as contribute to the increased energy production.

The neutronic calculations indicate that the blanket and shield chosen meet the guidelines discussed earlier. In addition, the blanket provides for excellent energy multiplication and possibilities for energy recovery. We shall optimize this basic design with the expectation of further improving the neutronic performance.

IV-D. Thermal Hydraulics

It has already been mentioned that the structural material selected for the TMR blanket is HT-9 and the breeding/cooling material is $Li_{17}Pb_{83}$. The basic blanket design is similar to that proposed for the initial Starfire blanket design. It consists of a series of tube banks running circumferentially around the central cell (Figure IV-2). Coolant/breeding material is manifolded at the top and bottom of the tubes and can be made to flow in either direction. MHD problems are not considered to be serious because of the low magnetic field and the small plasma radius.

The MHD pressure drop in the tubes can be easily calculated and is ~0.35 MPa. Suppression of turbulence by MHD effects is not expected to have a major effect on the heat transfer because the energy is primarily generated within the coolant. The temperature difference between the structure and the coolant will be minimal because the heat does not flow through the tube walls. The neutronic heating rates within the blanket are used to calculate the thermal hydraulics characteristics and these are summarized in Table IV-1.

Figure IV-2

CROSS SECTION OF CENTRAL CELL (UW TMR)

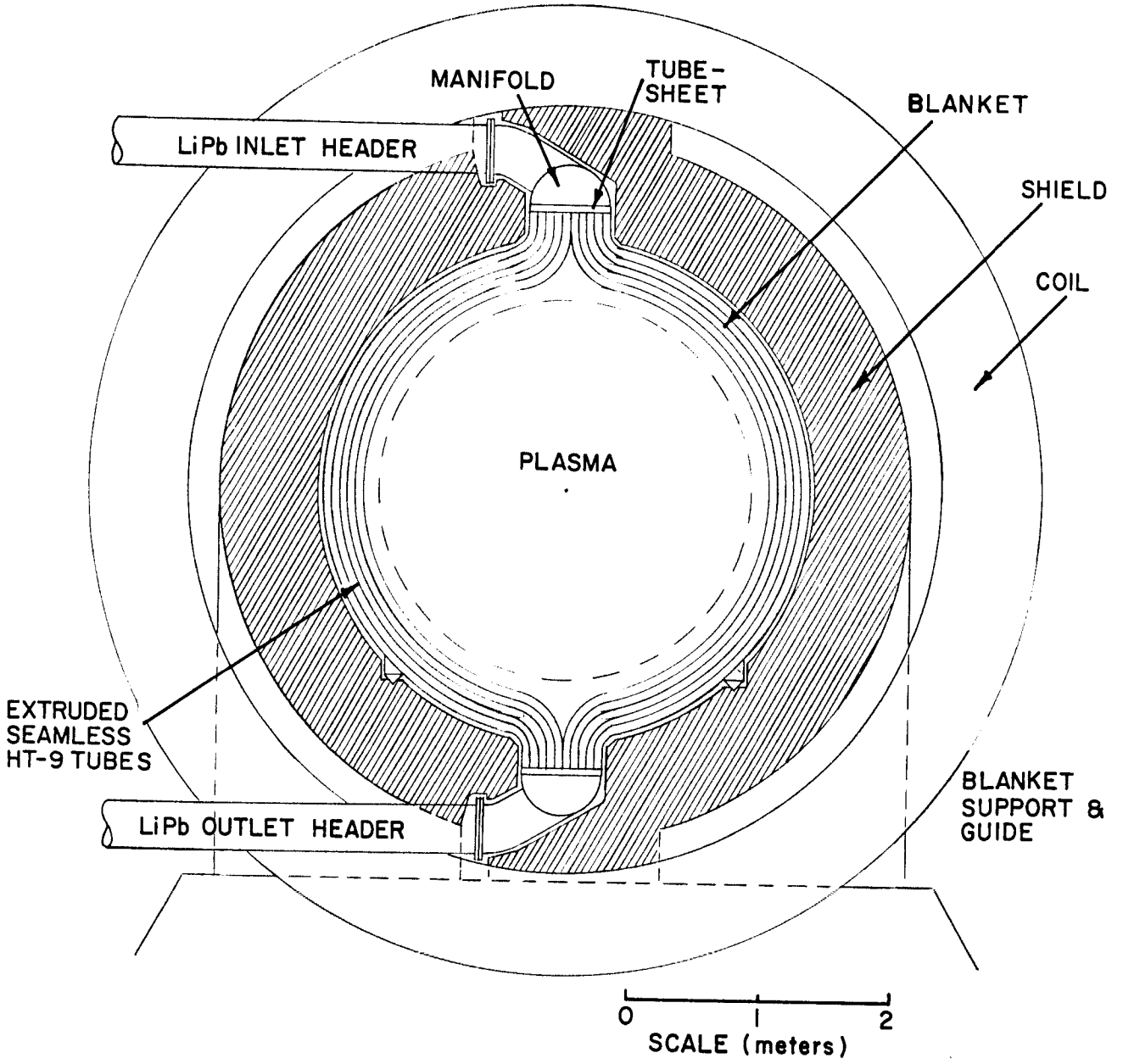

Table IV-1

Major Thermal Hydraulic Parameters (Preliminary)

Total Blanket Power	3216 MW
Neutron Wall Loading	2.7 MW/m^2
First Wall Heating Load	5 W/cm^2
Maximum Blanket Heat Deposition	24.4 W/cm^2
Blanket Composition	
HT-9	5%
$Li_{17}Pb_{83}$	95%
Coolant Temperature	
Inlet	329°C
Outlet	500°C
Maximum Structure Temperature	500°C
Maximum Coolant Velocity	17 cm/sec
MHD Pressure Drop	.35 MPa
Maximum Blanket Pressure	.7 MPa
Total Coolant Flow Rate	1.52×10^8 kg/hr
Steam Conditions	
Temperature	468°C (875 °F)
Pressure	165 MPa (2000 psi)
Reheat Temperature	299°C (510 °F)
Gross Thermal Efficiency	42%
Estimated Net Efficiency	37%

IV-E. Mechanical Design and Maintainability

The TMR blanket consists of banks of seamless tubes running circumferentially around the plasma in the central cell. Figure IV-2 shows a cross section of the blanket. The blanket in the central cell will be divided into modules, the length of which will depend on the separation between central cell magnets. The tubes in each module will be welded to tube sheets at the top and the bottom of the central cell. These tube sheets are in turn welded to semi-cylindrical manifolds which distribute the coolant uniformly among the tubes. Each module will have a single supply and a single return header attached to the manifolds at the top and bottom as shown in Fig. IV-2. This design provides the flexibility of running the coolant from the top to the bottom or vice-versa. Since radiation damage, in particular swelling, is a strong function of the temperature of the structure, the capability of periodic reversal of the coolant flow might mitigate the problems of radiation damage.

The tubes which will be ~10 cm in diameter can be either circular or square with rounded corners. Obviously the square tubes will have a smaller void fraction while the round tubes will have lower stresses. Either of these shapes will be easy to fabricate and lend themselves very well to mass production.

The blanket will not have a separate first wall. Instead, the first row of tubes will constitute the first wall. As shown in Fig. IV-3, the first row of tubes in the case of the square geometry can have the side facing the plasma remain cylindrical.

Fabrication of blanket modules will be relatively easy. The prebent tubes will be assembled together in a special fixture which will keep them assembled throughout fabrication. The tube sheets will then be

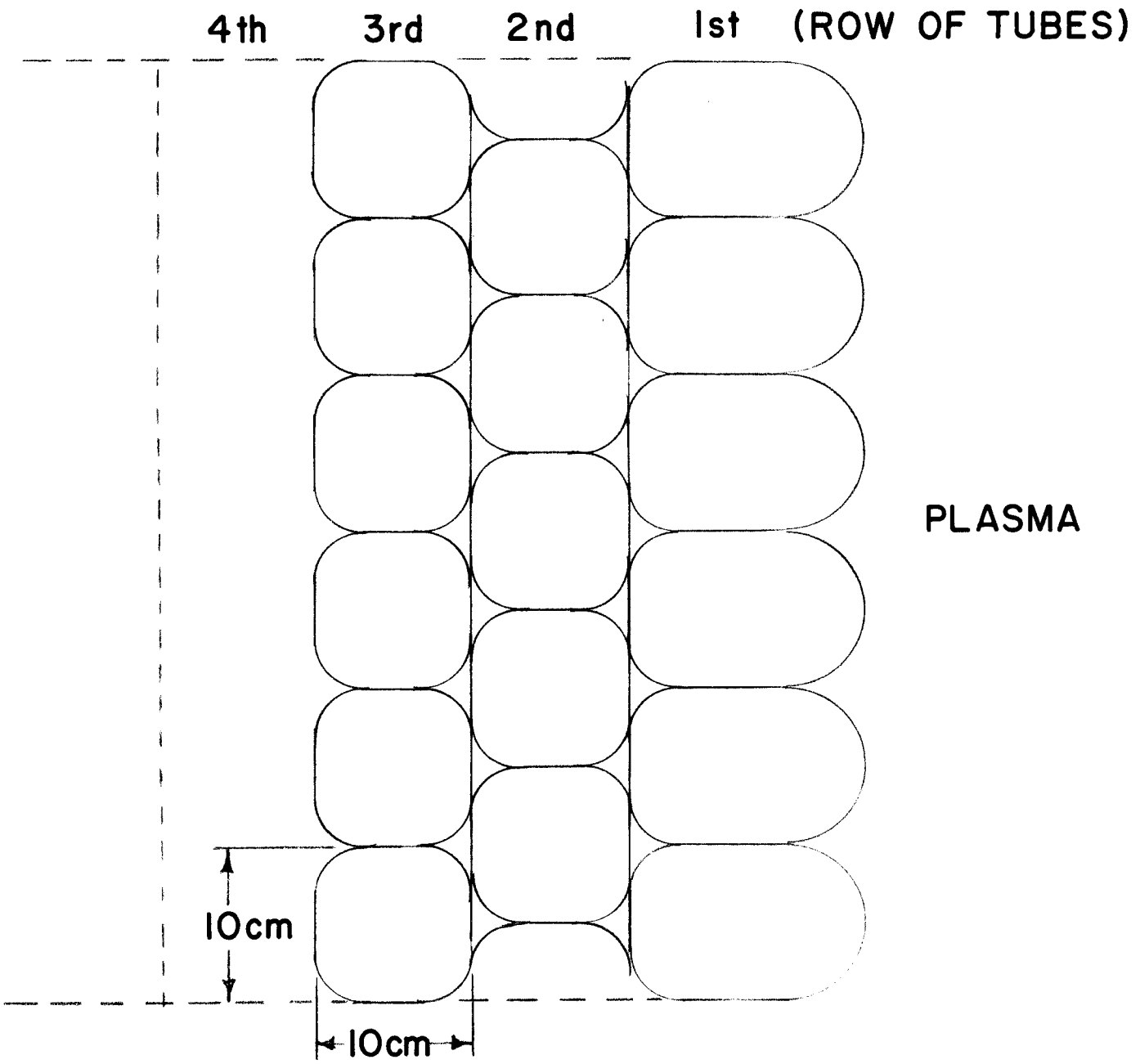

Figure IV-3. Schematic of Blanket Tube Sheet for Tandem Mirror Reactor.

welded to the tubes and then to the manifolds. The assembled module will then undergo an annealing operation to relieve the stresses due to welding. Each module can then be leak checked with a mass spectrometer and subsequently tested at high pressure and temperature in simulated operating conditions. In this way each module will have been tested very thoroughly prior to its assembly within the reactor.

The outstanding features of this blanket design are the following:

1. No welds exposed to a high radiation environment.
2. Low stresses.
3. Ease of fabrication, assembly and testing.
4. Capability of coolant flow reversal.
5. No separate first wall.

The maintainability of such a blanket has been carefully considered. As shown in Fig. IV-2, the blanket modules are supported on the shield by means of struts welded to the last bank of tubes. These struts are also used to guide the blanket modules axially through the shield in the central cell. Access points strategically distributed along the central cell will allow the blanket modules to be removed upward between central cell magnets. These access points will have the upper half of the central cell shield segments removable. Removal of a blanket module will necessitate the following steps:

1. Draining out of the coolant/breeding material
2. Disconnecting the supply and return headers and pulling them back to provide clearance.
3. Axial translation of the module to an access point along the central cell.
4. Lifting the module out by means of an overhead crane.

The major disadvantage of this maintenance scheme, is that removal of a failed blanket module may necessitate the preliminary removal of several other blanket modules. This drawback, however, will not affect routine maintenance procedures in which a block of modules will be replaced anyway.

IV-F. Tritium Considerations

The Wisconsin tandem mirror reactor is attractive from the standpoint of tritium handling in the fueling and exhaust cycles due to the high fractional burnup, pellet fueling and the use of hydrogen in the end plugs. The high burnup (31%) in the central cell results in only 1.1 kg/d of tritium exiting the reactor chamber, with a correspondingly low cryopump inventory on the order of tenths of kilograms. The quantity of tritium in storage is also low since this number is tied to the fractional burnup. A day's reserve of tritium (that quantity of tritium fed into the reactor on a daily basis) is only 1.6 kg. Pellet fueling of the central cell circumvents the problems of tritium handling associated with neutral beam injectors, namely the large tritium inventory and flow rate needed because of the low injector efficiency. (Generally only 1/8 to 1/10 of the gas supplied is actually injected.) Finally, the use of hydrogen in the end plugs is advantageous. Although the plug injection rate is only a few percent of the central cell fueling rate, the total gas associated with end plugs is not insignificant since the end plugs must be driven with neutral beams. Thus, if tritium instead of hydrogen is used in the end plugs, the tritium flow rate in the reactor would increase by 30%.

The attractive feature of the blanket is its low tritium inventory. The lithium activity in $Li_{17}Pb_{83}$ is only 1.3×10^{-4} at 500°C, and therefore the tritium is less tightly bound than in pure liquid lithium. (The

Sievert's constant is estimated to be 30,000 $torr^{1/2}$/mole fraction T in Li with the result that at a tritium pressure of 10^{-4} torr the tritium concentration is only 1 weight part per billion.) The blanket inventory is then on the order of grams and the total plant tritium inventory is roughly 2 kg.

However, the TMR also has some problems with respect to tritium. The need for large direct convertors to improve efficiency implies that there may be a large tritium inventory associated with them. Also the choice of a ferritic steel for the blanket and piping means that tritium diffusion through the structural material can be a problem. Permeability of tritium through ferritic steels at 400°C is 40 times higher than through stainless steel. Limiting the tritium loss to the steam in the power cycle to acceptable limits will require some ingenuity and is an area which will need further investigation.

IV-G. Structure Afterheat

The principal difference between HT-9 and 316 SS for the purpose of evaluating the activation of the structure is the elimination of the nickel isotopes and an increase in the amount of chromium. Calculations performed on preliminary blanket concepts tend to confirm that the net effect is rather small until very long times after shutdown. For example, the first wall activity of the HT-9 system relative to the 316 SS system is approximately 0.88 at shutdown; at one day following shutdown, 0.92; and at one year after shutdown 1.14. However, at 100 years after shutdown, the advantage for HT-9 goes to several orders of magnitude. Thus, it appears that as far as radioactivity is concerned, it is only from a long term storage standpoint that HT-9 appears to have an advantage.

References

1. S. N. Rosenwasser, P. Miller, J. A. Dalessandro, J. M. Rawls, W. E. Toffolo, W. Chen, First Topical Mtg. on Fusion Reactor Materials, Miami (1979).

2. B. A. Chin, et al., 9th ASTM Int. Symposium on Effects of Radiation on Structural Materials, Richland (1978).

V. Summary and Future Directions

The introduction of the thermal barrier has reduced considerably the technology requirements of the minimum-B plugs. Without the barrier, on-axis magnetic fields in the range of 10-14T were required to get a Q-value of 5 to 10. Furthermore the power density in the central cell was lower (~0.3 W/cm^3) and the wall loading was also low (~0.5 MW/m^2). With the barrier, it has been possible to reduce the min-B fields to 6T peak on-axis, and simultaneously, raise the central cell power density (6 W/cm^3), wall loading (2.7 MW/m^2), and Q (~33). This does not represent an optimized design, but only one possible configuration. The parameter space is rather extensive and there are many possibilities for trade-offs, but the relative costs and benefits of trading one parameter for another need to be quantified before a meaningful "optimum" can be found.

The introduction of the thermal barrier also presents some problems requiring solution. The particles trapped in the barrier have to be removed; one possibility is to use neutral beam pumping, as in the LLL reactor design. Another is to use drift orbit pumping, as suggested by Kesner. This method is about as energetically expensive as neutral beam pumping, but does not require the neutral beam hardware. Since it does not remove trapped particles from the center of the barrier cell and since ambipolar electric fields reduce the radial excursion of the drift orbit, its effectiveness is not yet established. It may need to be supplemented by additional methods.

The barrier cell also increases the possibility of MHD instabilities since it adds an additional region of bad curvature (combined with high mirror ratio), although the plasma pressure is small in this region. A possible fix is to add an additional min-B region inboard of the barrier cell in order

to add more good curvature and shorten the connection length. This increases the required field strength in the min-B magnets and lowers the overall-Q at a given central-cell beta, but may permit operation at higher beta.

Another possibility is to separate the function of generating the confining ambipolar potential from that of providing MHD stability. Generating the potential in a region different from the min-B MHD "anchor" allows for more flexibility which may bring with it improvements in the MHD stability and reduced magnetic field requirements.

It is concluded that if Yin Yang coils are required for TMR operation, it should be possible to design and construct Nb_3Sn coils, cooled with superfluid He and operating at $B_{max} \leq 15T$. It was found that copper stabilizers are preferred over Al stabilizers because of the high stresses in such coils even though there are many other potential advantages of Al.

The favorable geometry, the low heat load to the first wall and a uniformly low magnetic field in the central cell have allowed us to devise a rather attractive blanket configuration. The straight, central cylindrical geometry has made it possible to design a blanket which uses liquid $Li_{17}Pb_{83}$ in seamless, extruded tubes of a ferritic steel. The ferritic steel is chosen because of its resistance to radiation damage in fission reactors. The removal of welds to an easily heat treatable area as well as shielding them from the neutron flux should make the design more credible than for tokamak systems.

The use of $Li_{17}Pb_{83}$ solves many of the safety problems associated with liquid lithium and it also allows extremely low inventories of tritium in the blanket (e.g., less than 100 grams). In addition, the pumping of liquid metals in a low (~3-4 T) field can be accomplished with a relatively low fraction of the reactor output power.

The removal of blanket modules is also made simpler by the liquid metal approach. After draining the blanket modules, they can be easily removed from the cylindrical central cell section and replaced with no additional welding. This will greatly enhance the availability of the central cell region.

Finally, the overall safety of the UW-TMR design is expected to be much better than past reactor designs because of the low tritium inventory and because of the ease with which components can be remotely replaced.

The emphases in our design work in the near future will be in the following areas:

(1) Investigation of the effect of improved MHD configurations (such as the double min-B barrier-plug) on the overall reactor characteristics and technology requirements.

(2) More detailed analysis of the effectiveness of drift orbit pumping in the barrier cell.

(3) A more systematic parametric study of reactor performance with a view towards optimization.

(4) Development of a relativistic hot plasma description of the electron absorption processes for ECRF.

(5) Design of improved ERCF launching system considering the technological problems of a reactor environment.

(6) Analysis of tritium extraction from $Li_{17}Pb_{83}$ alloys and the permeability of tritium through HT-9 heat exchanger tube walls.

(7) Analysis of heat and neutron wall loading in the end plug regions.

(8) More complete neutron analysis for penetrations in the TMR.

(9) Development of the direct convertor portion of the reactor.

(10) Investigation of the vacuum pumping requirements for the UW-TMR.

(11) Analysis of the effect of magnetic steel on overall reactor design with particular attention paid to field calculations and support structures for components traversing from high to low magnetic field regions.

(12) A further investigation of the effects of neutron irradiation on HT-9 and its compatibility with Pb alloys.

(13) Safety analysis of the single heat exchanger approach.

(14) More detailed design of blanket modules consistent with heat removal and distribution of stresses.

(15) Investigation of potential new end plug magnet designs with particular emphasis on realistic stress levels in the structure, insulator and stabilizer regions.

(16) Design of central cell magnets which are consistent with rapid replacement of blanket and shield modules.

(17) Cost studies to determine the economic impact of end plug magnet structure on the total cost of the TMR.

In order to focus the future investigations we have established a "first cut" on the reactor design parameters. These are listed in Table V-1 and will be expanded in the next few months. It is felt that the parameters in Table V-1 are generally consistent with the goals we outlined for this program in section I of this report.

Table V-1

UW TANDEM MIRROR REACTOR PRELIMINARY DESIGN

Overall Parameters	
Thermal Power (Nominal)	3000 MW
Net Electric Power	1397 MW
Net Electric Efficiency	36.6 %
Reactor Q-Value	33
Neutron Wall Loading	2.7 MW/m^2
Central Cell Length	92 m
Central Cell Radius	1.3 m
Overall Length	118 m
Plasma Parameters	
Central Cell Density	1.1×10^{14} cm^{-3}
Central Cell Ion Temperature	40 keV
Central Cell Beta	.5
Plug Density	2.5×10^{13} cm^{-3}
Plug Ave. Ion Energy	980 keV
Plug Beta	.64
ECRH Power (@56 GHz)	25 MW
Neutral Beam Power	9.2 MW
Neutral Beam Energy	500 keV
Barrier Pump Power	56 MW
Power Density-Central Cell	6.2 W/cm^3
Magnet Parameters	
Plug Maximum Field (on axis)	6 T
Plug Mirror Ratio	1.5
Barrier Mirror Ratio	10
Maximum Barrier Field	15 T
Central Cell Field	3 T
Barrier Length	5 m
Transition Length	5 m
Blanket & Shield Parameters	
Reactor Structural Material	HT-9
Reactor Coolant	$Li_{17}Pb_{83}$
Breeding Ratio	1.13
Maximum Structure Temperature	500°C